MATEC Web of Conferences **31**, 01004 (2015)
DOI: 10.1051/matecconf/20153101004
© Owned by the authors, published by EDP Sciences, 2015

Secondary doping in polyaniline layers coated on multi-walled carbon nanotubes

Yi Zhou [1,a] , QingHua Song[1], WenYi Li [1]

[1] *The University of Toledo, USA Department of Biological Engineering, Xiangxi National Vocational-Technical College, Jishou, Hunan, China*

Abstract. HCl doped coaxial polyaniline/multiwalled carbon nanotubes (MWCNTs) nanocomposites were first prepared by in–situ chemical polymerization of aniline monomers in the presence of MWCNTs with less structural defects. P-toluene sulfonic acid (TSA) and 5-sulfosalicylic acid dihydrate (SSA) redoped PANI/MWCNT nanocomposites were achieved after the as-prepared nanocomposites were treated by ammonia respectively. The redoped nanocomposites were characterized by field emission scanning electron microscopy, transmission electron microscopy, fourier transform infrared spectroscopy, Raman, X–ray diffraction, thermogravimetric analysis and cyclic voltammetry, respectively. The results indicated that the thermal stability and electrochemical behaviour of TSA doped PANI/MWCNT nanocomposites were better than that of SSA doped PANI/MWCNT nanocomposites.

1 Introduction

Polyaniline (PANI) is one of the widely used conducting polymers due to its electronic, electrochemical, good environmental and thermal stability[1-5]. By using carbon nanotubes as templates, very high specific surface area of polymer layers can be obtained, especially the free N–H environment and quinoid units along the PANI backbone, the high electrochemical performance can be obtained when PANI were coated on the surface of the CNTs [6,7]. In this work, multi–walled carbon nanotubes (MWCNTs) with significantly less structural defects was effective templates for preparing redoped nanocomposites [8]. P–toluene sulfonic acid (TSA) and 5-sulfosalicylic acid dihydrate (SSA) redoped PANI/MWCNT nanocomposites through a sequential doping–dedoping–redoping process were prepared, then thermal stability and electrochemical behaviour of both redoped nanocomposites would be investigated.

2 Experimental methods

2.1 Materials

Commercial MWCNTs (purity ≥ 95 wt %, 20~40 nm in diameter, 5~15 μm in length, CVD method) were purchased from Shenzhen Nanotech Port Co. Ltd. Hydrochloric acid (HCl) and ammonia (NH4OH), acetone, p-toluene sulfonic acid(TSA) and 5-sulfosalicylic acid dihydrate (SSA) were obtained from Sinopharm Chemical Reagent Co. Ltd. Aniline monomers with a molar mass of 93 g/mol and a density of 1.02 g/cm^3 were purchased from Pinghu Chemical Reagent Co. Ltd., and used as received without any further purification. Ammonium peroxydisulfate (APS) were provided from Guoyao Group Chemical Reagent Co. Ltd. The deionized water was used for all the experiment.

2.2 Preparation

1 g MWCNTs were added to 300 ml of concentrated hydrochloric acid, and then treated at 80℃ with reflux reaction under ultrasound for 15 h. The treated MWCNTs with minimal defects were used as templates [6]. HCl doped nanocomposites were prepared by in-situ chemical oxidation polymerization of 1.2 g aniline monomer dispersed in 50 ml 1 M hydrochloric acid solution, and the product was named as MCPN-HCl. Then the MCPN-HCl was treated in ammonia solution, and sequently immersed into 100 ml TSA and SSA in aqueous solution under ultrasonic dispersion for 3 h at room temperature respectively, and the treated nanocomposites were named as MCPN-TSA and MCPN-SSA. After being washed by alcohol and deionized water, all the nanocomposites were vacuum dried at 80 ℃ for 48 h.

2.3 Characterization

The morphologies of two nanocomposites were observed on a HITACHI S–4800 field emission scanning electron microscopy (FE-SEM) and H-800 (Hitachi) transmission electron microscopy (TEM). The microstructures were characterized on a Nicolet 8700 Fourier transform

[a] Corresponding author: zhouyicynthia@126.com

This is an Open Access article distributed under the terms of the Creative Commons Attribution License 4.0, which permits unrestricted use, distribution, and reproduction in any medium, provided the original work is properly cited.

infrared (FT–IR) spectrometer with a resolution of 4 cm–1 over 32 scans. Raman spectra were recorded by a Renishaw spectrometer witha 50 mW Ar+ laser. The crystalline structures were characterized on a RIGAKU D/Max–2550 PC X–ray diffraction (XRD) instrument. The thermal stability was evaluated on a NETZSCH TG 209 F1 thermogravimetric analyser (TGA) at a heating rate of 10 ℃/min under nitrogen stream with a flow rate of 15 ml/min. The cyclic voltammogram (CV) was recorded on a CHI 1000A electrochemical working station (CH Instrument, Inc.) in 0.1 M H_2SO_4 aqueous solution by using a Pt wire as the counter electrode and Ag/AgCl as the reference electrode.

3 Results and Discussion

3.1. Morphology

Figure 1 shows the FE-SEM images for MCPN-TSA and MCPN-SSA nanocomposites. Both MCPN-TSA and MCPN-SSA nanocomposites exhibited uniform core–shell structure with larger tube diameter, which indicated the uniform formation of PANI layers on the surface of carbon nanotubes. Moreover, it can be observed that the surface of the nanocomposites by using SSA as the dopant was more roughness than that for TSA as dopant, as the doping anion size affects the entire nanocomposite size; the diameter of size was much bigger of the MCPN-SSA than that of MCPN-TSA.

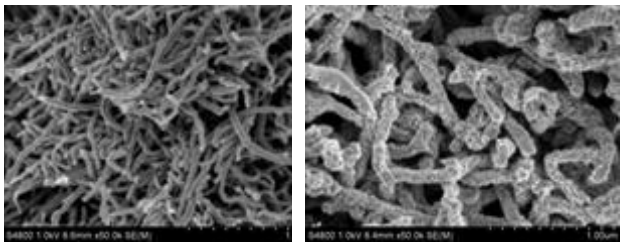

Figure 1. FE－SEM images of **MCPN**-TSA (left) and MCPN-SSA (right) nanocomposites

.

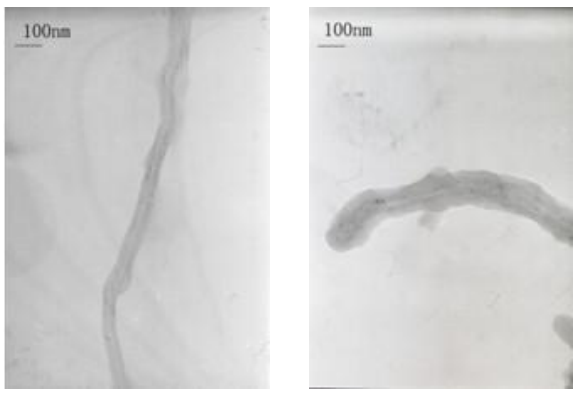

Figure 2. TEM images of MCPN-TSA (left) and MCPN-SSA (right) nanocomposites.

Figure 2 shows the TEM images for MCPN-TSA and MCPN-SSA nanocomposites. The carbon nanotubes and the polyaniline as core-shell structure were clearly exhibited in the images; even the interface between carbon nanotube and polyaniline was clearly showed. The diameter of MCPN-TSA was about 50nm, and the diameter of MCPN-SSA was about 90 nm, which much larger than that of MCPN-TSA and in accordance with the conclusions of FE-TEM.

3.2 Chemical Structure

The typical FT-IR spectra of MCPN-TSA and MCPN-SSA were displayed in Figure 3. The main bands situated at 820 cm^{-1}, 1120 cm^{-1}, 1235 cm^{-1}, 1280 cm^{-1}, 1500 cm^{-1}, and could be observed for all the nanocomposites, and these spectra were agreed with previously reported results [6,7]. The absorption band situated at 1120 cm^{-1} for MCPN-TSA shifts to higher frequency and observed less strengthened for MCPN-SSA, and the absorption band situated at 1500 cm^{-1} for MCPN-SSA shifts to higher frequency and showed less strengthened for MCPN-TSA. Such strong characteristic band is considered to be a measurement of delocalization of electrons, and a decrease in the intensity of such band indicates the existence of the weaker π–π* interaction in the composite.

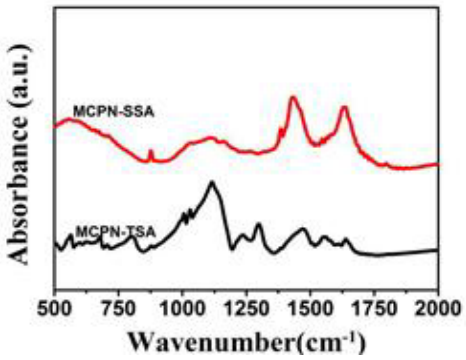

Figure 3. FT–IR spectra for MCPN-TSA and MCPN-SSA nanocomposites.

The typical Raman spectra of MCPN-TSA and MCPN-SSA were displayed in the next Figure 4. Compared with the pure PANI, the intensity of the peak at the 1163cm-1 was enhanced obviously, which meant that conjugate interaction between MWCNTs and PANI had led to increase the concentration of the corresponding quinone ring. The peak which located at 1495cm^{-1} was corresponding quinone imine, exhibited a relatively wide spectral band for both nanocomposites.

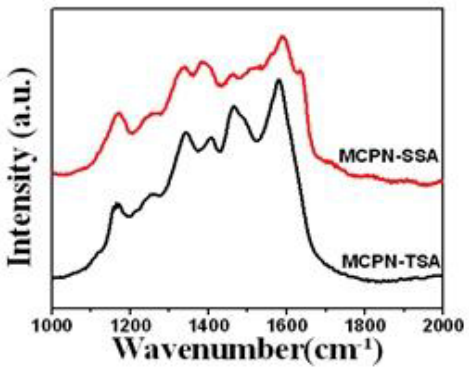

Figure 4. Raman spectra for MCPN-TSA and MCPN-SSA nanocomposites.

The x–ray diffraction patterns of the composites were shown in Figure 5. The main diffraction peak corresponding to pure carbon nanotubes was appeared at 25.88°, and the main diffraction peak corresponding to pure PANI was appeared at 24.80°. Carbon nanotubes play the role of nucleus, and aniline was using carbon nanotubes as support and polymerization slowly around it during the in-situ polymerization. It can found that the peak appeared in the 25.88° clearly, which meant the carbon nanotubes were stable in the nanocomposites. In addition, no diffraction peak of polyaniline and carbon nanotube was observed, which confirmed between conjugated polymers and carbon nanotubes was a kind of physical interaction, no chemical change was existed once again.

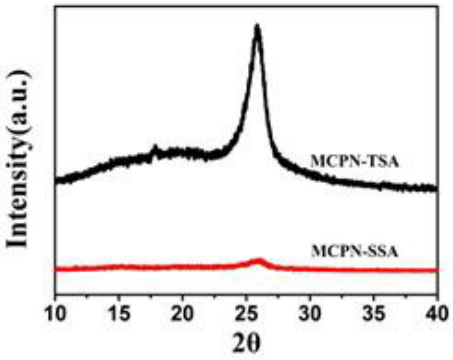

Figure 5.XRD spectra for MCPN-TSA and MCPN-SSA nanocomposite

3.3 Thermal Stability

Figure 6 illustrates the TGA curves for TSA doped and SSA doped PANI/MWCNT nanocomposites. With the increasing of the temperature, a significant decomposition below 250℃ could be observed for both nanocomposites, which was assigned to the volatilization of water and hydrochloric acid. Then an obvious different in the decomposition could be found when the temperature exceeded 300 ℃. For the MCPN-TSA, the weight dropped to 62.5% at 500 ℃ and 57.5 % at 800 ℃, whereas for MCPN-SSA, 61% at 500 ℃ and 50% at 800 ℃, which could be contributed to different the doping anion size, and strong interaction existed between PANI and both nanocomposites.

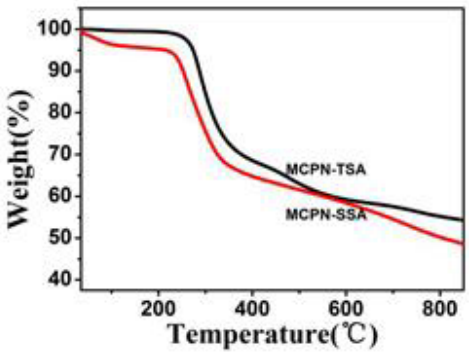

Figure 6.TGA curves for MCPN-TSA and MCPN-SSA nanocomposites.

3.4 Electrochemical Behaviour

The electrochemical properties of coaxial nanocomposites were evaluated by cyclic voltammetry. Figure 7 displays a study of the cyclic voltammetry for TSA doped and SSA doped nanocomposites measured at different scan rate in the 0.5 M H2SO4 aqueous electrolyte. It can be found that the CV curve for both nanocomposites exhibited a nearly rectangle shape, which indicated an ideal supercapacitor behavior, whereas the specific capacitance of MCPN-TSA was about 420.80 F/g at the scan rate of 1 mV/s, and larger than 265.85 F/g for MCPN-SSA, and the specific capacitance of MCPN-TSA was about 138.93 F/g at the scan rate of 5 mV/s, and larger than 107.87 F/g for MCPN-SSA.

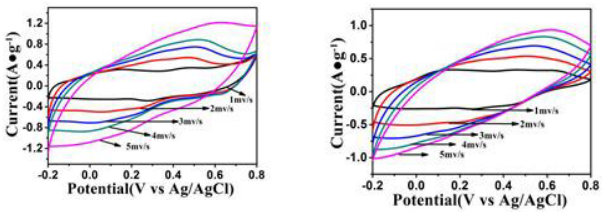

Figure 7.CV curves for MCPN-TSA (left) and MCPN-SSA (right) nanocomposites in 0.1M H2SO4 electrolyte at different scan rates

4 Conclusions

TSA and SSA redoped PANI/MWCNT nanocomposites were obtained by a sequential doping–dedoping–redoping process for HCl doped nanocomposites by covering PANI on the MWCNTs with less structural defects. It is found that although the both nanocomposites kept similar core–shell structure, the surface of the nanocomposites by using SSA as the dopant was more roughness than that for TSA as dopant. Moreover, TSA redoped nanocomposites exhibited better thermal stability and

electrochemical behavior compared with the nanocomposites redoped by SSA.

5 Acknowledgement

This work is supported by grant 15C1366 of the Hunan Provincial Education Department Foundation in China.

References

1. Xie H. Ma Y, Guo J, Synthetic Metals**123**,47–52 (2001)
2. Krinichnyi V. Roth H, Schrödner M. Wessling B, Polymer **47**, 7460–7468(2006)
3. Li T. Qin Z. Liang B. Tian F. Zhao J. Liu N. Zhu M, Electrochimica Acta **177**,343–351(2015)
4. Inigo AR. Henley SJ. Silva SRP, Nanotechnology **22**, 265711–1–6(2011)
5. Bounioux C. Katz EA. Yerushalmi-Rozen RC, Polymers Advanced Technologies**23**,1129–1140 (2012)
6. Li L. Qin ZY. Liang X, The Journal of Physical Chemistry C **113**, 5502–5507(2009)
7. Zhou Y. Qin ZY. Li L, Electrochimica Acta **55**, 3904–3908(2010)
8. Fan QQ. Qin ZY. Liang X, Journal of Experimental Nanoscience **5**, 337–347(2010)